Pergamon

Cement and Concrete Research 32 (2002) 1053–1059

CEMENT AND CONCRETE RESEARCH

Prediction of cracking within early-age concrete due to thermal, drying and creep behavior

Y. Yuan*, Z.L. Wan

Department of Building Engineering, Tongji University, Shanghai 200092, People's Republic of China

Received 2 May 2000; accepted 14 January 2002

Abstract

To predict potential early-age cracking after concrete placing, a numerical simulation procedure has been completed based on a micromechanical model and empirical formulas on the property development of young concrete. The numerical model could account for the effects of hydration, moisture transport and creep. Environmental influences, such as removal of formworks, curing conditions and variations of surrounding temperature and relative humidity, have been investigated. In calculating stress field with age caused by these synthetic physical–mechanical processes, three-dimensional finite element and finite difference (3D-FE-FD) methods are combined together.

Keywords: Concrete; Numerical simulation; Drying; Shrinkage; Creep

1. Introduction

It is well known that continuously casting concrete may result in cracking propagation within structures. Researchers and engineers have noticed that high thermal stresses happen within mass concrete members when pouring a thick foundation base or constructing a dam. Preventive measures, such as using less quantity and low-heat cement, adding proper additives, cooling down, insulating surface and placing rebars, had been developed since the middle of the past century. Wang and Dilger [1] compiled a program to predict temperature distribution in hardening concrete, and RILEM recently published a proceeding to summarize such works [2].

Recently, rapid and massive placing of wall/slab type structure as a whole has become more common due to advanced concrete pumping techniques. Cracking in this situation, unavoidably, becomes a main concern. Meanwhile, evidences showed that occurrence of cracks may be controlled through detailed preparations. Although microcracks cannot be prevented completely, the methodology to have it under control, however, is still unavailable.

* Corresponding author. Tel.: +86-21-6598-0234; fax: +86-21-6598-6345.

E-mail address: yuany@tongji.edu.cn (Y. Yuan).

Generally, early-age deformation in young concrete leads to excessive distortions, damage and even cracking. Subsequently, problems were encountered, such as deterioration in structural integrity, waterproof requirement and high costs in repair or replacement. Concrete deformation must be supported as far as possible by the quantification of its intensity and spatial distribution. Stress states resulting from deformations and long-term evolution of early-age reaction are the main consideration.

Simple empirical equations have been used in the past for estimation of the shrinkage of concrete. Roelfstra and Salet [3] completed a model to describe heat and moisture transport. Jonasson et al. [4], based on some essential models, studied early features of moisture and thermal effects and set up a linear relationship between shrinkage and relative humidity. Sellevold [5] summarizes Norway's results on a number of investigation. These approaches are easy to apply. A suitable and precise prediction approach involving structural detail, time-dependent variation, environmental conditions, and evaluation of stress distributions within structures would be expected. Bazant [6,7] gave a general concept on numerical simulation of concrete material and a series of publications focused on the microcracking mechanism according to fracture mechanics.

The major task here is to develop an accurate and applicable prediction method for structural behaviors suffer-

0008-8846/02/$ – see front matter
PII: S0008-8846(02)00743-3

ing from early-age reactions. The methodology should be in accordance with the following requirements: (a) The effects of concrete materials and mix proportions on drying shrinkage were to be considered in terms of differences in pore structures. (b) Variations in boundary and environmental conditions, including temperature, humidity, support and load, together with the curing conditions, were also to be considered. (c) Prediction of fields of thermal, moisture and deformation with age was needed. To satisfy these requirements, a macroscopic moisture distribution model had been combined with a micromechanical drying shrinkage model.

A theoretical numerical modelling procedure, based on the characteristics of concrete at both material level and micromechanical level, has been developed to simulate the whole process after concrete setting. Transient temperature and relative humidity fields and their influence to stress (strain) field of cast structure must be exactly matched. A compiled three-dimensional finite element and finite difference (3D-FE-FD) program conforms to this complex time-dependent process including thermal expansion, drying shrinkage and creep behavior. To verify the effectiveness of the proposed numerical procedure, a comparison with specific shrinkage test results is presented and a good agreement was obtained.

2. The mathematical model

For computational purposes, any point is subjected to three-dimensional strain. To predict the response of structure member in the early period of construction, a step-by-step method is necessary. At the beginning of each time step, deformation due to thermal variation (hydration and environment), drying shrinkage and creep during the current time interval is imposed. This imposed incremental strain on any point at ith time interval is defined as (Eq. (1))

$$\Delta\varepsilon_i^{\mathrm{ToT}} = \Delta\varepsilon_i^{\mathrm{sh}} + \Delta\varepsilon_i^{\mathrm{th}} + \Delta\varepsilon_i^{\mathrm{cr}} \tag{1}$$

where, $\Delta\varepsilon^{\mathrm{sh}}$ is the shrinkage strain at time t_i, $\Delta\varepsilon^{\mathrm{th}}$ is the thermal strain, $\Delta\varepsilon^{\mathrm{cr}}$ is the creep strain, and the ith interval is the one between setting time $(i)t$ and $(i+1)t$.

2.1. Strains due to thermal variation

The volume response of a concrete element subject to thermal effect is assumed to be linear (Eq. (2))

$$\varepsilon_T = \alpha\Delta T \tag{2}$$

where α is called the thermal dilation coefficient (TDC). The amount of work reported in the literature on the TDC of young concrete is quite limited and, hence, no conclusive behavior can be given at present. The general agreement on the TDC is that it depends on the moisture state of the matrix pore system [8]. For simplicity, it was assumed to be constant here (1.0×10^{-5}/K).

2.2. Strains own to drying shrinkage

Mechanism of shrinkage is far more complicated. Empirical equations have been widely used in numerical calculation. Many researchers mentioned the relationship between pore structure and moisture transportation. Shimamura suggested a theoretical micromechanical drying shrinkage model of concrete related with pore structure model [9].

There are various kinds of pores within the actual concrete. To accurately predict complicated aspects of the drying shrinkage of concrete, a simple formula is suitable for computation. The characterized pore structure model of concrete plays a major role in the proposed stress analysis of a structure. It assumes the density distribution function of pore size to be taken as (Eq. (3)) [9]

$$V(r) = V_0[1 - \exp(-Br^C)] \tag{3}$$

where the pore radius r is defined as one-half of the distance between the solid wall of a pore, V_0 is total volume of pores per unit concrete volume (m^3/m^3) and B and C are parameters that determine the configuration of the pore size distribution.

3. Modeling of microscopic phenomena in concrete

3.1. Thermodynamical equilibrium of vapor and liquid water

Without considering adsorption and adhesive wetting of water molecules on solid capillary walls, the relation of the equilibrated partial pressure of vapor in fine pores and the interface between the gas and liquid phases can be described by the Kelvin equation (Eq. (4)):

$$\ln h = \ln\frac{p_{\mathrm{V}}}{p_{\mathrm{V0}}} = -\frac{2\gamma M_{\mathrm{W}}}{RT\rho_{\mathrm{L}}}\frac{1}{r_s} \tag{4}$$

where p_{V} is the partial pressure of vapor (Pa), p_{V0} is the saturated partial pressure of vapor (Pa), $p_{\mathrm{V}}/p_{\mathrm{V0}}$ equals to relative humidity h, M_{W} is the molecular mass of water (kg/mol), R is the gas constant (J/mol K), T is the absolute temperature (K) and ρ_{L} is the density of liquid water (kg/m^3).

3.2. Stress due to capillary tension

Capillary theory stated that tensile stress is caused by the pressure difference between the gas and liquid phases [10]. This stress acts on pore walls and results in the shrinkage of concrete. The total intensity of the tensile stress per unit concrete volume will depend on both the magnitudes of the tension and the area where it is applied (Eq. (5)). That is

$$\sigma_s = A_s\frac{2\gamma}{r_s} \tag{5}$$

where σ_s is the capillary stress (Pa) and A_s is the representative area, which is expressed as the volume of liquid water per unit concrete volume V_L at the simplest level of assumption (Eq. (6)):

$$A_s = V_L \tag{6}$$

3.3. Deformation due to capillary stress

Capillary stress as defined here is different from the usual stress in its mechanism of generation. However, shrinkage deformation is expected to have similar characteristics as ordinary deformation, because it was a deformation of hardened cement paste. In this study, a simple linear elastic relationship was assumed as (Eq. (7)):

$$\varepsilon_{sh} = \frac{\sigma_s}{E_s} \tag{7}$$

where E_s is the elastic modulus for capillary stress (Pa).

4. Constitutive relationships

4.1. Heat diffusion within concrete

After concrete is placed in the field, it will be sustained in a thermal environment different from mixing. At early age, a great deal of heat will be generated with the hydration of cement. With day after night, temperature would be varied with time. With the help of heat conduction theory, heat diffusion within concrete is easily expressed in a differential equation (Eq. (8)):

$$\frac{\partial}{\partial x}\left(k_x\frac{\partial T}{\partial x}\right) + \frac{\partial}{\partial y}\left(k_y\frac{\partial T}{\partial y}\right) + \frac{\partial}{\partial z}\left(k_z\frac{\partial T}{\partial z}\right) + \frac{f(t)}{c\gamma} = \frac{\partial T}{\partial t} \tag{8}$$

where T is temperature of concrete (K), k_x, k_y and k_z are the diffusion ratios along the three different directions, c is the specific heat ratio (J/kg K) and γ is the density of concrete (kg/m^3). For simplicity, it was reasonably assumed that k_x, k_y and k_z are equal and constant. The function $f(t)$ describes heat generation from hydration, which can be simply expressed as follows (Eqs. (9) and (10)) [1,11]:

$$f(t) = \frac{\partial F(t)}{\partial t} = mWQ_0\exp(-mt) \tag{9}$$

and

$$F(t) = WQ_0(1 - \exp(-mt)) \tag{10}$$

where W is the cement content per unit volume (kg/m^3), Q_0 is the heat per unit cement content (J/kg), m is the hydration rate.

Boundary conditions around a given structure may be summarized with a simplified form (Eqs. (11) and (12)):

$$\text{At boundary } S_1\text{: } T(x,y,z,t) = T_0 = \text{const} \tag{11}$$

$$\text{At boundary } S_2\text{: } k_x\frac{\partial T}{\partial x}l_x + k_y\frac{\partial T}{\partial y}l_y + k_z\frac{\partial T}{\partial z}l_z + \beta(T - T_\infty) = 0 \tag{12}$$

where β is the relative diffusion ratio, which is determined by boundary types, curing conditions and other factors.

4.2. Moisture diffusion within concrete

Compared to heat diffusion, moisture content diffusion is more complicated due to the complex pore structure within concrete. As stated before, many investigators suggested different ways in simulating the moisture field. Nevertheless, Bazant's [6] proposed differential equation with respect to relative humidity is easy to be accepted, since it theoretically describes the process in three dimensions (Eq. (13)):

$$\frac{\partial}{\partial x}\left(k_x\frac{\partial h}{\partial x}\right) + \frac{\partial}{\partial y}\left(k_y\frac{\partial h}{\partial y}\right) + \frac{\partial}{\partial z}\left(k_z\frac{\partial h}{\partial z}\right) + k_h\frac{\partial q}{\partial t} + k_T\frac{\partial T}{\partial t} = \frac{\partial h}{\partial t} \tag{13}$$

where h is the pore moisture content volume per unit concrete volume (m^3/m^3), k_x, k_y and k_z are the diffusion ratios, T is the temperature, k_h and k_T are the two coefficients to reflect the hydration and temperature effects on the moisture content separately. For simplicity, it was assumed that k_x, k_y and k_z are equal and can be described as a function of $D(h)$. In CEB-FIP ('90) model code (1993), for isothermal conditions, the moisture coefficient $D(h)$ is expressed as a function of the pore relative humidity $0 < h < 1$ (Eq. (14)). Accordingly,

$$D(h) = D_1\left(\alpha + \frac{1-\alpha}{1 + [(1-h)/(1-h_c)]^n}\right) \tag{14}$$

where D_1 is the maximum of $D(h)$ for $h = 1.0$, $\alpha = D_0/D_1$, D_0 is the minimum of $D(h)$ at $h = 0.0$, h_c is the pore relative humidity at $D(h) = 0.5D_1$ and n is an exponent. $\alpha = 0.05$, $h_c = 0.80$ and $n = 15$ are approximately assumed. D_1 may be estimated from Eq. (16)

$$D = \frac{D_{1.0}}{f_{ck}/f_{ck0}} \tag{15}$$

where $D_{1.0} = 3.6 \times 10^{-6}$ m^2/h, $f_{ck0} = 10$ MPa and the characteristic compressive strength f_{ck} (Eq. (15)) may be estimated by the mean compressive strength f_{cm}, i.e., $f_{ck} = f_{cm} - 8.0$ (MPa).

Pertinent boundary conditions can be assigned at a different region (Eqs. (16) and (17)):

$$\text{At boundary } S_1\text{:}\quad h(x,y,z,t) = h_0 = \text{const} \tag{16}$$

$$\text{At boundary } S_2\text{:}\quad k_x \frac{\partial h}{\partial x} l_x + k_y \frac{\partial h}{\partial y} l_y + k_z \frac{\partial h}{\partial z} l_z + g(h,h_\infty) = 0 \tag{17}$$

and the modified Menzel's equation gives out function $g(h,h_\infty)$ (Eq. (18))

$$g(h,h_\infty) = A(0.253 + 0.06\nu)(h - h_\infty) \tag{18}$$

where A is an empirical coefficient, ν is average wind speed (m/s).

4.3. Creep of concrete

One of the main characteristics of concrete that distinguishes it from the traditional viscoelastic materials is the time-dependent effect. Experiments indicated that deformation response due to a load increment is independent of all other past load increment. This implies the applicability of superposition principal. Thus, for small increments in stress vector $\{d\sigma\}$ occurring at time t measured from setting time (Eq. (19))

$$\varepsilon(t) = \int_0^t [J(t,t')]\mathrm{d}\sigma \tag{19}$$

At interpretation of this creep stress–strain law, numerical analysis can be performed by subdividing the total time interval into time multisteps λt at discrete times t_r ($r = 1, 2, \ldots$). Then, the integral can be approximated through finite summation of involved stress incremental over the whole time interval. To avoid the difficulty in computing sums involving total stress history, a series of real exponential would be used as an approximated replacement of the creep function (Eq. (20))

$$J(t,t') = \frac{1}{E(t')} + \sum_{i=1}^{n} \frac{1}{\hat{E}_i(t')}\{1 - \exp[-(t - t')/\tau_i]\} \tag{20}$$

where τ_i are constraints called retardation times and E_i is an aging coefficient.

A complete stable incremental analysis was proposed by Bazant [6] with the assumption that $\{d\sigma\}/dt$ and $E_i(t')$ are constant within each time interval ($t_{r-1} < t < t_r$). The incremental stress–strain law becomes (Eqs. (21)–(23))

$$\{\Delta\sigma\}_r = E''_r[\bar{D}](\{\Delta\varepsilon\}_r - \{\Delta\eta\}_r) \tag{21}$$

in which

$$\frac{1}{E''_r} = \frac{1}{E_{r-0.5}} + \sum_{i=1}^{n} \frac{1 - [1 - \exp(-\Delta t_r/\tau_i)]\tau_i/\Delta t_r}{(\hat{E}_i)_{r-0.5}} \tag{22}$$

and

$$\{\Delta\eta\}_r = \sum_{i=1}^{n} [1 - \exp(-\Delta t_r/\tau_i)]\{\varepsilon_i{}^*\}_{r-1} \tag{23}$$

The effect of prior stress histories is contained in the set of vectors $\{\varepsilon_i{}^*\}$, which is defined by the recurrence formula (Eq. (24))

$$\{\varepsilon_i{}^*\}_r = \frac{\{\Delta\sigma\}_r[1 - \exp(-\Delta t/\tau_i)]\tau_i/\Delta t_r}{(E_i)_{r-0.5}} + \{\varepsilon_i{}^*\}_{r-1}\exp(-\Delta t_r/\tau_i) \tag{24}$$

where the coefficients $E_i(t')$ are restricted to the form

$$\frac{1}{E_i(t')} = a_i + b_i(t')^{n_i} \tag{25}$$

where a_i, b_i and n_i are material constants (Eq. (25)).

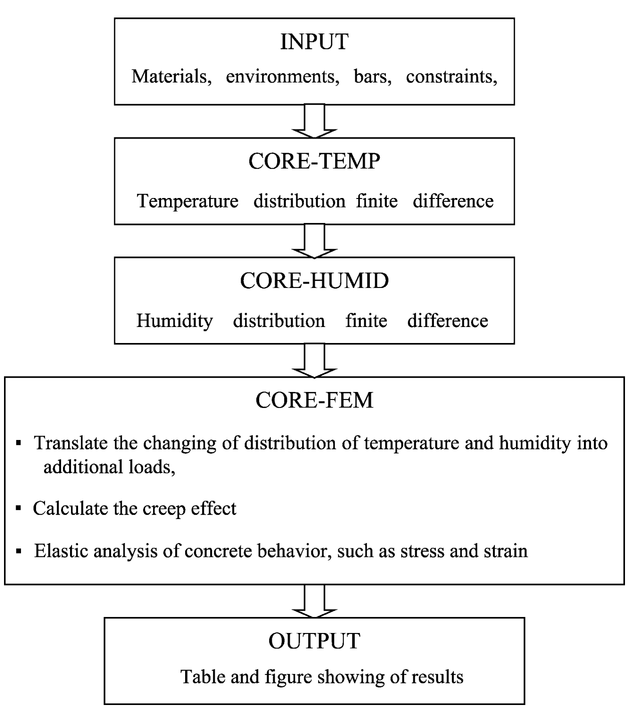

Fig. 1. Flow chart of CCC program.

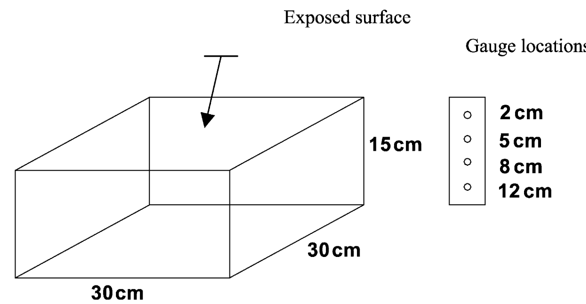

Fig. 2. Geometry and size of specimen.

Table 1
Mix proportions of concrete

Specimen	w/c (%)	s/a (%)	Unit weight (kg/m^3) Water (w)	Cement (c)	Sand (s)	Gravel (g)	Admixture	f_c (MPa)
Mix I	65	42	202	310	740	1020	–	28
Mix II	40	38	172	430	661	1079	1.0	44

4.4. Age-dependent properties of concrete

In calculating and analysing the behavior of premature concrete, age-dependent properties of concrete must be taken into consideration to avoid imprecision, since prominent variances happen in them with the cement hydration procedure. To consider all the factors consistently and simply, we suggested the empirical model of development in cement hydration, which was utilized to define and describe other aging properties, such as strength, elastic modulus, moisture diffusion coefficient, pore size distribution parameter, etc. The hydration rate was defined as follows (Eqs. (26)–(28)):

$$H(t) = \frac{t}{C + Dt} \tag{26}$$

$$f_c(t) = H(t) f_c(28) \tag{27}$$

$$E_c(t) = \sqrt{H(t)} E_c(28) \tag{28}$$

where t is current age (in days), and $f_c(28)$ and $E_c(28)$ are the 28-day strength and elasticity modulus, respectively. The relationship between f_c, E_c and age was recommended by Grzybowski and Shah [12].

5. Numerical implementation

A three-dimensional numerical program CCC (Concrete Cracking Control) has been developed for the above nonlinear analysis of concrete. An eight-node serendipity isoparametric element coped with the effects of reinforcement is assumed. At each node of an element, three degrees of freedom are specified, corresponding to three displacements at that node. Stress and strain are evaluated at Gauss integration points within each element. The program is compiled in the format of Visual C++ code as organized in the flow chart in Fig. 1.

Table 2
Physical constants used in study

Molecular weight of water, M_W	0.01802 kg/mol
Gas constant, R	8.31453 J/mol K
Density of liquid water, ρ_L	1000 kg/m^3
Surface tension of liquid water, γ	0.0727 N/m

Table 3
Input data

Specimen	V_0	$B(28)$	E/E_s
Mix I	0.24	38,000	3.5
Mix II	0.22	45,000	3.5

6. Verification

6.1. General

The proposed model was verified based on the experimental data presented by J.-K. Kim and C.-S. Lee [13], which was used to verify the prediction of differential drying shrinkage of some specific concrete specimens.

6.2. Outline of the experiments

The specimens as shown in Fig. 2 were exposed to a constant-temperature and constant-humidity room of 20 ± 1 °C

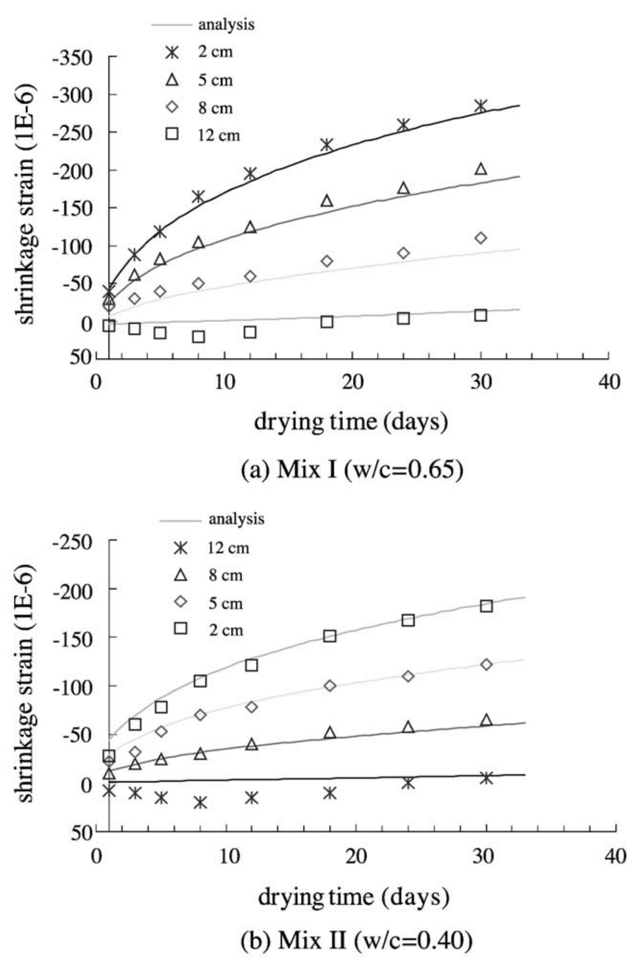

Fig. 3. Shrinkage strain development with age.

and 68 ± 2% RH after moist curing for 7 days. Five sides of the specimen were sealed with paraffin wax to ensure the uniaxial moisture diffusion. The embedded strain gauges were installed at distances of 2, 5, 8 and 12 cm from exposure surface to measure the internal concrete strain. Detailed concrete mix proportions are given in Table 1.

6.3. Analysis and comparison

The physical constants used in this study are shown in Table 2. In the proposed model, the material characteristics are represented by four parameters: V_0, the initial total volume of pores per unit concrete volume; $B(28)$ and C, parameters that determine the configuration of the pore size distribution; and E_s, the elastic modulus for capillary stress. As suggested in the study of Shimomura and Maekawa [9], C can be set to 0.5, and the ratio of E to E_s, elastic modulus for concrete, is between 2 and 3. The input data used in this paper are listed in Table 3.

Because of no boundary restraint, the creep effect was not taken into consideration. As shown in Fig. 3, the analytical results of the differential drying shrinkage are in good agreement with test results. Other analytical results were shown in Figs. 4 and 5. In the results of relative humidity distribution, we can find that due to extremely lower transportation coefficient of concrete material, the core of specimen still keep high humidity after a long time. Here, self-desiccation was not taken into consideration. Also, stress results show that although there were no strong boundary restraints, differential shrinkage according to the depth results in relative high tensile stress exists near the exposure surface, which is self-balanced by internal compression and causes the microcrack of concrete surface directly. Since the material properties are assumed as elasticity in this study, it could not account for fracture properties. To predict young concrete reactions precisely, further research needs to be developed to take crack behavior into consideration.

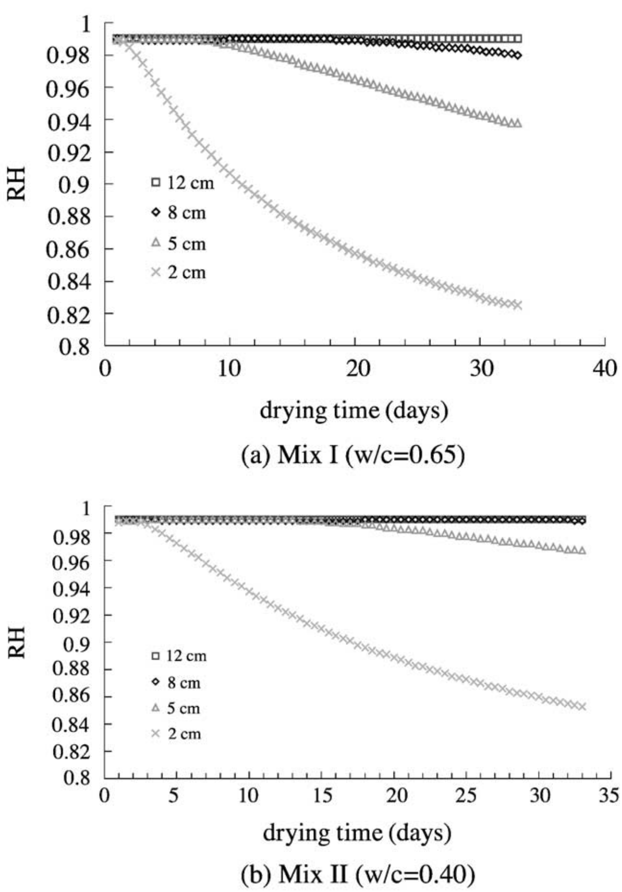

Fig. 4. Relative humidity development with age.

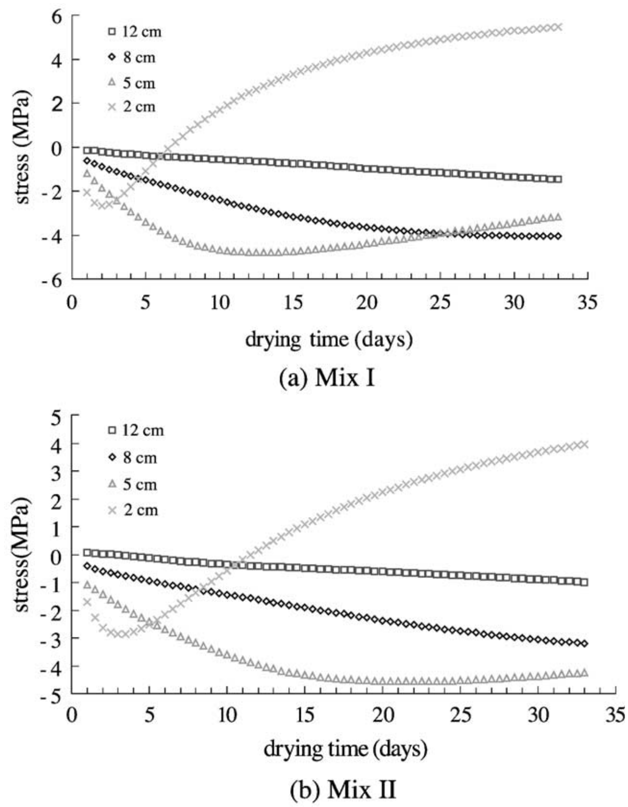

Fig. 5. Stress development with age.

7. Conclusions

This paper proposed an analytical model to predict potential cracking of early-age concrete. The model could account for the effects of hydration, moisture transport and environmental influences. Verification states the following conclusions.

1. The analytical model proposed here incorporates many of the key influential parameters governing the performance of premature concrete and enables

simulation and prediction of development in drying shrinkage and thermal expansion in young concrete under various conditions.

2. The good agreement between analytical results and tests shows that the modelling of pore structure within concrete is adequate in predicting the drying shrinkage behavior.
3. Significant variances of the internal drying shrinkage strain according to the depth from drying surface result in large tensile stress directly, even surface cracking.
4. Further research needs to be done to analysis the postcracking behavior within young concrete.

Acknowledgments

The research presented here was partially supported by the Natural Science Foundation of China (Grant No. 59778031). The authors also appreciate the comments and help of Professor David A. Lange, University of Illinois at Urbana-Champaign.

References

[1] Ch. Wang, D.H. Dilger, Prediction of temperature distribution in hardening concrete, in: R. Spingenschmid (Ed.), Thermal Cracking in Concrete at Early Ages, E & FN Spon, London, 1994, pp. 21–28.

[2] R. Spingenschmid (Ed.), Thermal Cracking in Concrete at Early Ages (RILEM conference), E & FN Spon, London, 1994.

[3] P.E. Roelfstra, T.A.M. Salet, Modelling of heat and moisture transport in hardening concrete, in: R. Spingenschmid (Ed.), Thermal Cracking in Concrete at Early Ages, E & FN Spon, London, 1994, pp. 37–44.

[4] J.E. Jonasson, P. Groth, H. Hedlund, Modelling of temperature and moisture field in concrete to study early age movements as a basis for stress analysis, in: R. Spingenschmid (Ed.), Thermal Cracking in Concrete at Early Ages, E & FN Spon, London, 1994, pp. 45–52.

[5] E.J. Sellevold, High-performance concrete: Early age cracking, pore structure, and durability, in: V.M. Malhotra (Ed.), High Performance Concrete (ACI SP-172, Proceedings of the Third ACI International Conference), Kuala Lumpur, Malaysia (Production: Julie Carpenter) pp. 192–208.

[6] Z.P. Bazant, Mathematical Modelling of Creep and Shrinkage of Concrete (RILEM Series), Wiley, London, 1982.

[7] Z.P. Bazant, Interaction of fracture and creep in concrete, Cem. Future 6 (1) (1994) 4–5.

[8] A.M. Neville, Properties of Concrete, fourth ed., Wiley, New York, 1996.

[9] T. Shimomura, K. Maekawa, Analysis of the drying shrinkage behaviour of concrete using a micromechanical model based on the micropore structure of concrete, Mag. Concr. Res. 49 (181) (1997) 303–322.

[10] J.F. Young, The microstructure of hardened Portland cement paste, in: Z.P. Bazant (Ed.), Creep and Shrinkage in Concrete Structures, John Wiley & Sons, Chichester, 1988, pp. 3–22.

[11] T.M. Wang, Control of Cracking in Engineering Structure, third ed., China Architecture and Building Press, Beijing, 1997 (in Chinese).

[12] M. Grzybowski, S.P. Shah, Model to predict cracking in fiber reinforced concrete due to restrained shrinkage, Mag. Concr. Res. 41 (148) (1989) 125–135.

[13] J.-K. Kim, C.-S. Lee, Prediction of differential drying shrinkage in concrete, Cem. Concr. Res. 28 (7) (1998) 985–994.